European Journal of Pharmaceutical Sciences 186 (2023) 106463

Contents lists available at ScienceDirect

European Journal of Pharmaceutical Sciences

journal homepage: www.elsevier.com/locate/ejps

Polymer-embedded deep eutectic solvents (PEDES) as a novel bio-enabling formulation approach

Shaida Panbachi [a,b], Josef Beranek [c], Martin Kuentz [a,*]

[a] University of Applied Sciences and Arts Northwest. Switzerland, Institute of Pharma Technology Hofackerstr. 30, Muttenz CH-4132, Switzerland
[b] Institute of Pharmaceutical Technology, University of Basel, Klingelbergstrasse 50, Basel 4056, Switzerland
[c] Zentiva, k.s., U Kabelovny 130, 102 00 Praha 10, Czech Republic

ARTICLE INFO

Keywords:
Deep eutectic solvents
Low transition-temperature mixtures
Enabling formulation(s)
Precipitation inhibition
Molecular dynamics simulation(s)
Solubilizing carrier

ABSTRACT

There is a growing interest in using deep eutectic solvents (DES) as a pharmaceutical delivery system for poorly water-soluble compounds. To reduce the risk of drug precipitation following oral administration, this study addresses the hypothesis that directly including a polymeric precipitation inhibitor (PI) in a DES mixture could obtain a polymer-embedded deep eutectic system (PEDES) as a novel bio-enabling formulation principle. Following broad formulation screening, a PEDES embedding 15% w/w of polyvinyl pyrrolidone K30 (PVP) in L-carnitine:ethylene glycol (1:4, molar ratio) DES was successfully formulated as a supersaturating formulation using indomethacin as model compound. The drug solubility of 175.6 mg/mL obtained in DES was remarkably high, and upon release (phosphate buffer, pH 6.5) a maximum supersaturation factor of 9.8 was recorded, whereby the release kinetics displayed a suitable "parachute effect". The formulation was further characterized to include a molecular dynamics simulation. It can be concluded that PEDES appears to be a viable novel formulation approach, setting solid grounds for further research to assess the full potential of this novel type of supersaturating drug delivery system.

1. Introduction

To cope with poor aqueous solubility of novel drug candidates, so-called bio-enabling formulations are needed both to supply preclinical studies and provide a final drug product for the market (Shah et al., 2019). Various formulation principles have been evaluated over the years (Boyd et al., 2019; Sugano, 2012), and drug solubilization in co-solvent mixtures or lipids is a common approach (Buckley et al., 2013). There has also been much interest in pharmaceutical use of ionic liquids (Pedro et al., 2020). While the latter can exhibit outstanding drug solubilizing properties, there are also drawbacks such as the limited choice among toxicologically acceptable components for pharmaceutical use. It is only in recent years that a novel formulation type with similar solubilizing characteristics to ionic liquids has emerged. These so-called deep eutectic solvents (DES) (Abbott et al., 2002) have been claimed to be a less toxic, more environmentally friendly alternative to traditional ionic liquids (Fourmentin et al., 2021; Kaur et al., 2020). DES are defined as a mixture of components with hydrogen-bond donating and accepting properties, interacting at a specific molar ratio to give a significant reduction in melting point (Martins et al., 2019). These components are usually solids at room temperature and require activation energy to finally liquify as a mixture. Milling, extruding, mixing, or stirring accompanied with heating are examples of manufacturing techniques for such liquids. The components interact through hydrogen bonds, which are formed between the functional groups at various contact points of the components (Abbott et al., 2002). This results in a high-entropy state generating the liquid state (Abbott et al., 2002). DES have been shown to possess useful characteristics with a range of potential applications during pharmaceutical synthesis and drug product development. Some examples of DES applications in chemical production are as a solvent system to tailor the synthesis of polymeric drugs (García-Argüelles et al., 2013) and inorganic nanomaterials (Lee, 2017), or to control polymorphism of active pharmaceutical ingredients (API) (Potticary et al., 2020). DES have also been used as a medium for self-assembly of surfactants and lipids (Sanchez-Fernandez et al., 2018, 2021). Moreover, some studies have shown improved drug dissolution by incorporating an API as a building block in the DES (Aroso et al., 2016a). This is referred to as therapeutic deep eutectic solvents/systems (THEDES), where the API takes on the role of either the hydrogen bond donor or the hydrogen bond acceptor in the formulation (Fourmentin

* Corresponding author.
E-mail address: martin.kuentz@fhnw.ch (M. Kuentz).

https://doi.org/10.1016/j.ejps.2023.106463
Received 15 February 2023; Received in revised form 28 April 2023; Accepted 8 May 2023
Available online 9 May 2023

et al., 2021; Umerska et al., 2020). Some DES have shown improved bioavailability through increased permeability brought by some of the components incorporated (Aroso et al., 2016b; Chakraborty et al., 2021).

Most interestingly, DES have previously shown a several thousand-fold increase in solubilization for multiple organic compounds compared to other aqueous or organic media (Li & Lee, 2016). Particular model compounds in DES were, for example, rutin, berberine, curcumin and aprepitant (Faggian et al., 2016; Jeliński et al., 2019; Palmelund et al., 2021; Sut et al., 2017). These studies show the potential of DES as bio-enabling formulations due to their excellent solubilizing characteristics. However, there is clear demand for more drug delivery studies on DES, which has also been stressed in review articles (Chakraborty et al., 2021; Hansen et al., 2021). A recent study in the framework of DES as bio-enabling formulations was carried out by Palmelund et al. (2021), using aprepitant as a model of a poorly soluble API. The study compared *in vitro* and *in vivo* data obtained from the API-loaded DES to that of other established bio-enabling formulations, namely neat amorphous drug and a commercially available nanocrystalline aprepitant formulation. The DES formulation showed a higher oral bioavailability in rats than amorphous aprepitant, while comparable exposure was obtained with the nanocrystal formulation. This result is indeed promising for using DES-based formulations for oral delivery of poorly water-soluble drugs. DES formulations induce drug supersaturation upon *in vitro* dispersion in aqueous release media (Palmelund et al., 2021) and such concentration behaviour is also expected to occur *in vivo*. High initial supersaturation is especially observed on aqueous dispersion of liquid formulations, providing a strong driver of drug precipitation (Kuentz, 2019; Taylor & Zhang, 2016).

Therefore, this study explored the possibility of embedding a polymeric precipitation inhibitor (PI) in a DES to obtain a supersaturating drug delivery system (SDDS) showing adequate “spring & parachute” (Mathews & Sugano, 2010) progress of drug release. For such desirable release behaviour, apparent supersaturation is maintained for a longer period compared to that of polymer-free DES (Bauer-Brandl & Brandl, 2019; Bevernage et al., 2013). Precipitation is expected to occur in the release medium due to supersaturation generated by aqueous dispersion of an API solubilizing DES, which has also been observed in the work of Palmelund et al. (2021). However, it is important to note that this previous work did not embed a polymer in the formulation itself, but the excipient was added to the release medium. Embedding a polymer in DES has been previously attempted in fields outside of pharmaceutical technology, for example in chemical engineering (Rahma et al., 2017) and polymer physics (Sapir et al., 2016; Tomé & Mecerreyes, 2020). Recently proposed systems in which the polymer is a DES component itself (Rahma et al., 2017) are also an interesting focus, although these must be differentiated from the current work on incorporating polymeric precipitation inhibitors (PIs) in DES, for which we propose the name polymer-embedded DES (PEDES). Accordingly, an initial screening of polymer addition has been conducted to study at which concentration a PI can be solubilized in a DES without phase separation of any component. The present study further includes a model drug (indomethacin) and characterizes suitable model formulations to address the hypothesis that PEDES can be translated into a viable pharmaceutical formulation.

2. Materials and methods

The chemicals used in the study have been provided from various sources. Polyvinyl pyrrolidone K 30 (PVP), hydroxypropyl methylcellulose (HPMC), ethylene glycol, L-proline, levulinic acid, choline-chloride, DL-malic acid, oxalic acid, glycerol, xylitol, betaine, and glucose were purchased from Sigma-Aldrich (Merck KGaA, Taufkirchen, Germany). For the HPLC analysis and buffer preparation, acetonitrile 99.9%, glacial acetic acid 99.7%, sodium chloride 99.5% and sodium hydroxide 0.1 N were from Brunschwig (Appolo, Fluorochem, Chempur, Basel, Switzerland). For the Karl-Fischer titrations, Aquastar® solvent and Titrant 5 were purchased through Sigma-Aldrich (Merck KGaA, Taufkirchen, Germany). Further chemicals including L-carnitine, urea and indomethacin were purchased through Brunschwig (Appolo, Fluorochem, Chempur, Basel, Switzerland). The LMP grade hydroxypropyl methylcellulose acetate succinate (HPMCAS) was provided by Shin-Etsu (Shin-Etsu Naoetsu Plant, Joetsu, Japan).

2.1. Screening of pharmaceutically relevant DES found in literature

For the screening, systems were prepared using oven heating (Li & Lee, 2016). This method was applied for the preparation of 5 g DES in 20 mL glass vials (Schmidlin Labor & Service SA, Neuheim, Switzerland) in a heating oven without any stirring until a homogenous transparent liquid was formed. The systems that could be reproduced at a temperature of 80°C after a maximum of 16 h heating (without stirring) were selected for further screening.

2.2. Polymer solubility

The solubility of different polymers in the selected DES was determined by incremental addition of polymer until precipitation. The weight percentage of polymer added per weight of DES started from 2.5% w/w increasing in steps of 2.5% w/w until the solution became opaque. The maximum amount dissolved with the solution remaining transparent provided estimated polymer solubility. The polymers investigated were hydroxypropyl methylcellulose (HPMC), hydroxypropyl methylcellulose acetate succinate LMP (HPMCAS) and polyvinylpyrrolidone K30 (PVP). These were chosen based on their promising history of precipitation-inhibition function, as examples of classic polymeric precipitation inhibitors shown in literature (Bauer--Brandl & Brandl, 2019). DES with polymer was mixed on a magnetic stirrer at a rate of 300 rpm at 37°C and left to stir overnight for equilibration.

2.3. Preparation of shortlisted DES candidates

The batch-sizes of the final formulations were scaled up to 60 g. The components were mixed and heated on a magnetic stirring plate at 350 rpm and 80°C until a transparent liquid was formed (Abbott et al., 2002; Morrison et al., 2009). The transparent liquid was then dried in a vacuum oven at 100°C for 2.5 h. Lastly, the dried liquid was poured into a 100 mL crimp-top serum bottle and the vials were hermetically sealed with aluminium crimp seals with silicone septa. The bottles and the seals were purchased through Sigma-Aldrich (Merck KGaA, Taufkirchen, Germany).

2.4. Stability tests of selected candidates and API-incorporated final formulations

The DES candidates, either with or without polymer, were placed in two different relative humidity chambers at 20 and 40% humidity (Memmert GmbH & Co. KG, Schwabach, Germany), in both sealed and open 2 mL glass crimp vials with aluminium crimp caps (Wicom GmbH, Heppenheim, Germany). The same stability test was then performed for the final polymer-embedded candidates with the incorporated API. The changes in weight along with the visual changes in the physical state of the formulation were noted over 4 weeks and the experiments were performed in triplicate ($n = 3$).

2.5. Determination of thermodynamic solubility

Indomethacin was added in excess to DES for solubility testing. The mixture was mixed on a magnetic stirrer with a rate of 350 rpm (IKA® Werke GmbH, Staufen, Germany) for 24 h at a temperature of 37°C. The sample was transferred to 2 mL microcentrifuge tubes (Ratiolab GmbH,

Dreieich,Germany), centrifuged at 14,000 rpm for 30 min twice, and the resulting supernatant was filtered through a 0.45 μm HPLC-filter (17 mm Titan HPLC-filter, PTFE, Infochroma AG, Goldau, Switzerland). The solution was then diluted with a factor of 2000 in the mobile phase for indomethacin-content quantification using high-performance liquid chromatography (HPLC), as described in the section below. The experiment was performed in five replicas ($n = 5$).

2.6. Quantification of indomethacin using high-performance liquid chromatography (HPLC)

The indomethacin content of samples was determined using the Agilent 1260 Infinity II HPLC instrument (Agilent Technologies AG, Basel, Switzerland). The mobile phase was a mixture of acetonitrile and 0.1 M glacial acetic acid at a volumetric ratio of 70:30. A 4.6×100 mm C18 column was applied (InfinityLab Poroshell 120 EC-C18, Agilent Technologies AG, Basel, Switzerland); a flow-rate of 0.8 mL per minute was used during the separation in HPLC to detect indomethacin at a wavelength of 228 nm for evaluation on the Agilent OpenLAB CDS ChemStation software version 2.3.54 (Agilent Technologies AG, Santa Clara, USA). The calibration curve concentration range applied was 1 to 100 μg/mL. The calibration and the measurements were all performed in triplicate ($n = 3$).

2.7. Determination of water-content using volumetric Karl-Fischer titration (KFT)

Sample water content was determined using volumetric Karl-Fischer titration (Titrando 841 KFT-instrument, Metrohm Schweiz AG, Herisau, Switzerland). The titration factor was determined by the titration of 30 μL purified water using a 1 mL graduated calibrated microliter syringe (with cemented needle, Hamilton Storage GmbH, Domat, Switzerland) and Titrant 5 as the titrant. The prepared DES samples were diluted with methanol to give a solution with a concentration of 1 g/mL of water-containing-DES in solvent. A 1 mL plastic syringe (Injekt®-F Luer Solo syringe, B. Braun Medical AG, Sempach Switzerland) fitted with a needle (100 Sterican®, 20 G x 1 ½, B. Braun Medical AG, Sempach, Switzerland) was then used to inject 1 mL of the solution in the titration medium (Aqustar®, Merck KGaA, Taufkirchen, Germany). The water content and titration graph was then obtained by Tiamo software version 2.4 (Metrohm, Herisau, Switzerland). The measurements were performed in triplicate.

2.8. Water-binding patterns using time-domain ^1H nuclear magnetic resonance (TD-NMR)

The benchtop TD-NMR instrument (minispec mq20, Bruker, Rheinstetten, Germany) was employed to determine the binding patterns of water in DES. A set of DES with gradually increasing amounts of water ranging from 1 to 35% w/w were prepared for the analysis of the binding patterns. The TD-NMR was used particularly to determine the bound water population and the residual population of free water molecules in the bulk. This was measured using the ^1H spin-lattice relaxation time T1. A standard inversion recovery pulse sequence was applied $[RD - 180° - IR - 90° - RDT - asd]_{NS}]_N$, where RD denotes the recovery delay interval set to 1000 msec and IR is an incremented inversion recovery delay interval with the first pulse separation configured at 5 msec and the final pulse at 2000 msec. RDT depicts the delay for receiver dead time at 0.03 msec and asd is the sampling window, also at 0.03 msec. NS represents the number of scans for signal averaging (in this case NS = 8), and the N is the number of data-points collected, which was 20. Lastly, a biexponential decay function was used for data fitting to distinguish the two populations of water in the samples. The measurements were performed in quadruplicate ($n = 4$), and the obtained data was plotted against the total water content using GraphPad Prism software version 9.4.1 (GraphPad Software, California, USA).

2.9. Non-sink miniature-scale release study

Samples of 1 mL DES, with and without polymer, were mixed with indomethacin at 80% concentration of the equilibrium solubility value, which is a typical reference saturation level for comparison of different formulations in non-sink release testing. The samples were stirred at 37°C for 24 h in hermetically sealed 20 mL glass vials. The samples were then transferred to a pre-heated shaker at 37°C with an agitation rate of 450 rpm. A volume of 10 mL of pH 6.5 phosphate buffer was added to the glass vial in the oven at time point 0. The temperature of the oven was 37°C, in which the buffer, syringes and filters were pre-heated to maintain constant conditions during sample extraction. Samples were taken out at time-points 2, 5, 10, 15, 30, 60, 90, and 120 min, using a 1 mL syringe equipped with a needle to pierce the rubber septum of the vial. The sample was then immediately filtered through a 0.45 μm filter (17 mm Titan HPLC-filter, PTFE, Infochroma AG, Goldau, Switzerland) and diluted with the mobile phase described in Section 2.6. The quantities of indomethacin in solution at the given timepoints were then detected using HPLC at 228 nm, as described above, and plotted as a function of time. The non-sink miniature-scale release study was performed in triplicate for each formulation, and the data was evaluated using GraphPad Prism software version 9.4.1 (GraphPad Software, California, USA).

2.10. Rheometry

A controlled-stress rheometer (Modular Compact Rheometer MCR 302e, Anton Paar GmbH, Graz, Austria) was used to study the flow properties of formulation candidates, and data were evaluated in the RheoCompass™ software version 1.30. The software further estimated yield points calculated according to the Casson regression model (Kuentz et al., 2006). The studied samples were the DES with or without polymer, either loaded or free of API, in triplicate. Cone and plate with a diameter of either 50 mm in case of liquids or 25 mm in case of semi-solids was used for the measurements (CP50-1, Anton Paar GmbH, Graz, Austria). The temperature was kept constant at 25°C and the shear rates applied increased from 0.1 to 100 s^{-1}.

2.11. Molecular dynamics simulations

Molecular dynamics (MD) simulations were based on the YASARA software version 20.12.24 (YASARA Biosciences GmbH, Vienna, Austria) (Krieger & Vriend, 2014). Accelerated calculations were obtained by use of graphic processing units (GPUs) for calculation of the non-bonded interactions (Van der Waals and real-space Coulomb forces Krieger & Vriend, 2014). A general AMBER force field, GAFF2 was employed (Wang et al., 2004), wherein atomic charges were based on a semi-empirical quantum chemical estimation (AM1BCC) (Jakalian et al., 2002). The simplified solvent system consisted of 300 L-carnitine molecules and 1200 molecules of ethylene glycol to represent the composition of the finally selected DES vehicle. Moreover, ten oligomers of PVP (each consisting of 20 monomers) and 50 molecules of indomethacin were included in the solvent system, using a cuboid simulation box of 59×62×63 Å with periodic boundary conditions. Following steepest decent and simulated annealing minimizations to remove clashes, an initial simulation run at 600 K for 1 ns was conducted to remove any arbitrary oligomer orientation from initial placement. Subsequently, the main simulation was run for 10 ns at 298 K. Equations of motion were integrated with a 2×1.25 fs. A double time step was employed because of intermolecular forces are computationally expensive to calculate and change occurs more slowly over time. Thus, intramolecular forces were calculated every 1.25 fs, while intermolecular forces were calculated every 2.5 fs to provide a simulation step. An NTP ensemble was used where pressure control was achieved by rescaling the simulation cell

along the x,y, and z axis to reach a constant pressure of 1 bar. For temperature control, atom velocities were rescaled using a weakly coupling thermostat that kept the macroscopic temperature at the requested value. The software was not using the strongly fluctuating instantaneous microscopic temperature to rescale velocities at each simulation step (i.e., a classical Berendsen thermostat) but instead, a scaling factor was calculated according to Berendsen's formula from the time average temperature to avoid artifacts that are often observed with a classical Berendsen thermostat. A cut-off value of 8 Å was selected for the Van der Waals forces and the particle mesh Ewald algorithm was applied to electrostatic forces (Essmann et al., 1998).

2.12. Differential scanning calorimetry

The melting point of indomethacin was determined using the differential scanning calorimetry DSC 3 STAR^e system (Mettler Toledo, Greifensee, Switzerland). About 6 mg of indomethacin was weighed into a 40 μL aluminium pan and covered with a pierced lid of the same material. The nitrogen purge was set to 200 mL/min, and the heating rate to 5°C/min. Measurement consisted of two cycles ranging from 40 to 280°C. The thermograms were evaluated in the STAR^e Evaluation-Software version 16 (Mettler Toledo, Greifensee, Switzerland). The experiments were performed in triplicate.

3. Results and discussion

The hypothesis of whether or not it is feasible to produce a viable pharmaceutical PEDES was addressed first by the development process stages, starting with a series of DES formulations that were shortlisted to give a suitable candidate system for advanced characterization, as outlined in the following sections.

3.1. Screening

A series of potential DES mixtures was obtained from a literature study that focused on possible pharmaceutical usage. Moreover, the scope of the initial literature search was expanded to include other low-transition-temperature mixtures (LTTMs). The latter term includes mixtures for which a significant drop in glass transition temperatures is obtained (Francisco et al., 2013). Therefore, the current work uses the term "deep eutectic solvents" (DES) rather broadly for different systems that are scientifically relevant for pharmaceutical formulation development (Francisco et al., 2013). An initial broad screening of formulations used the oven method (Li & Lee, 2016) without stirring at a temperature of 80°C for 16 h for feasibility testing. As a result, 22 DES systems are listed in Table 1, for which the samples could be reproduced at the given conditions. The DES listed were considered to require less activation energy to mix than some other systems reported in the literature that may require more energy to form a DES (Fourmentin et al., 2021; Ramón & Guillena, 2019). The aspect of a comparatively lower activation energy of formation is beneficial regarding lean manufacturing or for inclusion of any thermolabile drug.

Avoiding heat stress on the formulation is not only beneficial regarding drug stability; a recent review points to the chemical stability of DES components and in particular, the choline chloride-based DES systems, are prone to esterification (Abranches & Coutinho, 2023). However, these systems have been widely used in literature, without taking the esterification into consideration (Abranches & Coutinho, 2023). Our work includes the choline chloride systems only in the initial screening phase, but they were not further studied together with other DES mixtures that could not dissolve the selected PIs, which is reported in more detail in the following section.

3.1.1. Polymer-embedded ethylene glycol-based DES

Polymers have frequently been used as PIs in SDDS (Warren et al., 2010) to facilitate the "spring and parachute" (Mathews & Sugano, 2010) progressive release described in the introduction. Examples of commonly used PIs include hydroxypropyl methylcellulose (HPMC), hydroxypropyl methylcellulose acetyl succinate (HPMCAS) and polyvinyl pyrrolidone (PVP) (Warren et al., 2010). The three polymers were tested in the 22 selected DESs listed in Table 1. The observation of opaqueness was defined as the cut-off point in the physical solubility test of the PI in DES. An initial amount of 2.5% w/w was tested to see if the polymer could be dissolved. As a result, none of the 22 selected DES could dissolve 2.5% w/w of the HPMC so this PI was not further considered within the present study. However, four of the 22 selected DES samples could dissolve varying amounts of both of the other candidate PIs, i.e., HPMCAS and PVP. The four systems capable of dissolving the highest amounts of both HPMCAS and PVP, were the L-carnitine:ethylene glycol (1:4) mixture, the glycerol:urea (1:1) mixture, or the L-proline systems with either ethylene glycol (1:3) or levulinic acid (1:2).The PVP showed generally higher solubility in the DES compared to the HPMCAS. The highest amount of HPMCAS that could be dissolved in all four of the aforementioned samples was 5% w/w. All the prepared HPMCAS samples apart from the L-proline:levulinic acid (1:2), turned into semi-solid gelled mixtures. In contrast, none of the viscous PVP mixtures formed a gel. Maximum PVP solubility was observed at 20% w/w in the glycerol:urea (1:1) mixture, whilst only 15% w/w could be dissolved in the rest. Accordingly, these four

Table 1
Overview of the literature-inspired DES reproducible in an oven heated to 80°C, without stirring.

Component 1	Component 2	Component 3	Molar Ratio	Refs.
Choline chloride	L-proline	DL-malic acid	1:1:1	(Ramón & Guillena, 2019)
L-proline	Oxalic acid	-	1:1	(Faggian et al., 2016)
L-proline	Levulinic acid	-	1:2	(Rahman et al., 2021)
L-proline	Ethylene glycol	-	1:3	Modified from (Şahin et al., 2023 n.d.)
Glycerol	L-proline	-	3:1	(Benvenutti et al., 2019)
L-carnitine	Ethylene glycol	-	1:2	(Zhang et al., 2017)
L-carnitine	Levulinic acid	-	1:2	(Huber et al., 2022)
L-carnitine	Ethylene glycol	-	1:4	(Marcus, 2019)
Choline chloride	Malonic acid	-	1:1	(Marcus, 2019)
Choline chloride	Xylitol	DL-malic acid	1:1:1	(Dai et al., 2013)
Choline chloride	DL-malic acid	-	1,5:1	(Dai et al., 2013)
Choline chloride	Glycerol	-	1:2	(Benvenutti et al., 2019)
Choline chloride	Ethylene glycol	-	1:2	(Marcus, 2019)
Choline chloride	Urea	-	1:2	(Abbott et al., 2002)
Glycerol	DL-malic acid	-	1:1	(Benvenutti et al., 2019)
Glycerol	Xylitol	-	1:1	(Skowrońska & Wilpiszewska, 2022)
Glycerol	Urea	-	1:1	(Skowrońska & Wilpiszewska, 2022)
Glycerol	Oxalic acid	-	1:1	Based on previous experiments from own archive
Betaine	Ethylene glycol	-	1:4	(Marcus, 2019)
Betaine	Levulinic acid	-	1:2	(Lu et al., 2016)
Betaine	DL-malic acid	L-proline	1:1:1	(Dai et al., 2013)
Betaine	Glycerol	Glucose	4:20:1	(Jeong et al., 2017)

formulation candidates were selected for further investigations, as they could dissolve targeted amounts of both PI polymers.

3.1.2. Initial physical stability testing

The stability of the DES can be compromised once an extra component is introduced to the system (Fourmentin et al., 2021; Marcus, 2019; Palmelund et al., 2021; Ramón & Guillena, 2019). It was therefore important to study the physical stability of a polymer-embedded DES (PEDES), to detect a potential phase separation. Therefore, 10 mL batches of the DES were mixed with each of the polymers (5% w/w of HPMCAS or 15% w/w PVP) and left for 4 weeks, at room temperature in a 20% relative humidity chamber. Any visual differences were noted to identify the physical changes within the given timeframe, and thereby providing information on the possible thermodynamic stability under these conditions. A low relative humidity of 20% was chosen as DES have been shown to exhibit hygroscopicity (Palmelund et al., 2021), which will be further discussed in Section 3.2. As a result, the most stable system was the polymer-embedded L-carnitine:ethylene glycol (1:4) DES. This system ranked first with respect to physical stability, and it should be mentioned that for a model research purpose, regulatory aspects of oral acceptance were not considered.

The next best formulation type regarding absence of any visual phase separation was the L-proline:ethylene glycol (1:3) mixture, which was stable over four weeks with the HPMCAS sample, whilst having a lower stability of under four weeks for the sample with PVP. The L-proline: levulinic acid (1:2) PVP-embedded system displayed stability of 2 weeks followed by the PVP-embedded glycerol:urea (1:1) sample with a stability of four days that was marked as the least stable, and hence the least likely sample to result in a viable pharmaceutical formulation.

The corresponding HPMCAS-embedded systems showed higher stability but for further experiments, only systems showing a promising stability with both of the two alternative polymers were targeted. Hence, the system showing the relatively highest stability with both polymers was L-carnitine:ethylene glycol (1:4) DES with either 5% w/w of HPMCAS or 15% w/w PVP, referred to as HPMCAS-PEDES and PVP-PEDES, respectively. In summary, the initial stability results obtained for the different PEDES are listed in Table 2.

3.2. Impact of water on shortlisted PEDES

Even though DES were initially thought to be much less hygroscopic than ionic liquids, their absolute tendency to adsorb water from the environment is still relevant (Fourmentin et al., 2021; Palmelund et al., 2021). The crucial solubilization property of the DES is highly dependent on the integrity of the DES (Fourmentin et al., 2021). Impurities in the DES, including water, would likely influence properties of the system, as new interacting components are introduced into the mixture. In this study, the binding patterns of water within a series of samples with different volumes of added water, were analysed using TD-NMR. The different ratios obtained were then plotted against the total amount of water as determined by Karl-Fischer titration (Fig. 1). This method is of interest because the water is believed to be primarily lodged in small nano-tubular structures within the DES (Fourmentin et al., 2021). The first layer of water interacting with the PEDES components would then be expected to consist predominantly of "bound" water molecules as they form a hydration layer. This is different from the water molecules floating within the confined nano-tubular structures, which contribute to the "unbound" water within the system. This would also mean that percolation can take place with a threshold concentration of water for which the nano-tubular structures form a coherent network in the sample (Abreu-Villela et al., 2019; Machado et al., 2016). The TD-NMR is a non-invasive technique measuring the amplitude of the two relaxation times $T1_1$ and $T1_2$ through spin-lattice relaxation times to represent the different water populations. The amplitudes recorded at the peaks obtained from the biexponential decay function from $T1_1$ and the $T1_2$ show the bound and unbound water populations, respectively (Kuentz et al., 2006).

The ratio of unbound to bound water is depicted as a function of the total amount of water in mass percentage in Fig. 1. The samples were analysed for the pure DES (L-carnitine:ethylene glycol (1:4)), the HPMCAS-PEDES and the PVP-PEDES. The total amount of water consists of the initial amount of water within the system, combined with added water ranging from 0.5% w/w to 35% w/w. For the pure DES, an increase in error bars can be seen for increasing amounts of water. A mechanism underlying this phenomenon could be percolation of water-containing nanostructures. A previous analysis in lipid-based formulations identified such percolation thresholds already at a few percent of water added (Machado et al., 2016). In DES, such a threshold of percolating nanostructures can be much higher because not all water may reside in nanostructures given the considerably more polar character of the components as compared to a lipid-based formulation. However, a quantitative analysis of percolation phenomena was beyond the scope of the present article and more details on percolation phenomena in pharmaceutics can be inferred from a recent review (Abreu-Villela et al., 2019). Fig. 1 further shows that beyond about 10% w/w total water the population of unbound water in the PVP-PEDES drifts in the direction of higher values compared to those of the pure

Table 2
Summary of the selected polymer soluble DES, and their stability.

DES (HBA: HBD (molar ratio))	HPMCAS concentration (% w/w)	HPMCAS-PEDES stability	PVP concentration (% w/w)	PVP-PEDES stability
L-carnitine: ethylene glycol (1:4)	5%	> 4 weeks	15%	> 4 weeks
L-proline: ethylene glycol (1:3)	5%	> 4 weeks	15%	< 4 weeks
L-proline: levulinic acid (1:2)	5%	2 weeks	15%	2 weeks
Glycerol: urea (1:1)	5%	2 weeks	20%	4 days

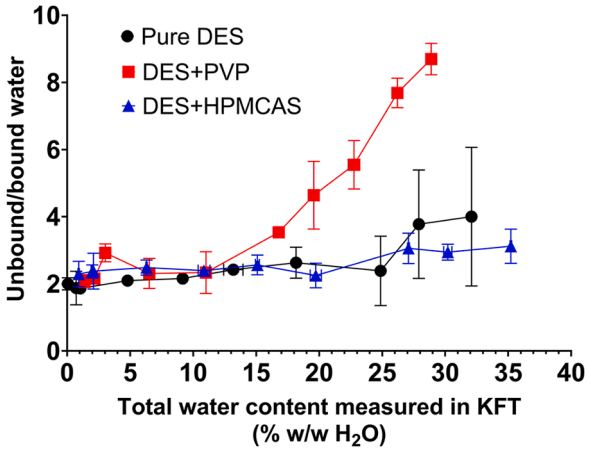

Fig. 1. Graph depicting two population types of water in the polymer-embedded formulation candidates, shown as the population of unbound to bound water measured using the time-domain NMR, plotted against increasing total water content (% w/w). The formulations evaluated were the pure DES, L-carnitine:ethylene glycol (1:4) (● *'pure DES'* black line on the graph), embedded with either 5% w/w HPMCAS (▲ *'DES+HPMCAS'* blue line on the graph), or 15% w/w PVP (■ *'DES+PVP'* red line). The trends show that with increasing amounts of water, an increased amount of unbound water is observed in the case of the PEDES ($n = 4$).

DES. PVP is known to be a hygroscopic polymer and will therefore surround the chains with water (Hiremath et al., 2019). Assuming that the polymer is more hygroscopic than the DES, an initial monolayer of bound water molecules followed by a pool of unbound water molecules will be in the immediate bulk phase around the polymer chains. By contrast HPMCAS-PEDES contained the notably less polar, and hence less hygroscopic, polymer compared to PVP and accordingly, the curve of the water ratios was very similar to that of pure DES (Friesen et al., 2008). As properties such as solubility are subject to change depending on the amount of water exposure, the DES was dried before the addition of polymer, and stored in hermetically sealed vials under controlled humidity environments to avoid risk of change in physicochemical properties by the interference of water. The drying step added to the production method in this section makes a difference to the method described in Section 3.1.2, which should avoid possible negative effects of water on phase behaviour or later on drug solubility (Abranches & Coutinho, 2023; Fourmentin et al., 2021; Palmelund et al., 2021).

3.3. Incorporation of API into shortlisted PEDES

Indomethacin was chosen as a model drug in our study, as it is grouped as a class II active pharmaceutical ingredient (API) in the Biopharmaceutical Classification system (BCS). Indomethacin is a non-steroidal anti-inflammatory drug (NSAID) with analgesic effects on local and systemic inflammatory diseases (Vranić & Uzunović, 2010). The solubility found for indomethacin in the selected DES, L-carnitine. ethylene glycol (1:4) was determined to be 175.6 ± 3.428 mg/mL, setting the baseline solubility in each of the PEDES formulations. The melting point obtained from a standard DSC measurement was 161.3 ± 0.2°C corresponding to the melting point of polymorph form 1 (Guo et al., 2011). The solubility value of 0.0011 mg/mL of indomethacin in water at 37°C has been previously reported in literature (Shakeel et al., 2013) while the solubility value of indomethacin measured in phosphate buffer pH 6.5 was found to be 0.562 ± 0.005 mg/mL. Clearly, great solubilization was observed in the DES with improved solubility that stretched to a magnitude of several thousand folds compared to the aqueous solubility of indomethacin at 37°C. To formulate the polymer-embedded and API-containing DES, a concentration corresponding to 80% DES-saturation was selected arbitrarily (i.e., 140.5 mg/mL). Knowledge of the drug solubility value at 37°C is relevant for release testing as the initial supersaturation prior to drug precipitation is defined.

3.3.1. Rheology

The viscosity for the pure DES sample was 0.148 ± 0.002 Pa•s, 2.69 ± 0.12 Pa•s in the PVP-embedded DES and 422.9 ± 48.6 Pa•s in the HPMCAS-embedded DES, measured at the shear rate of 0.1 s^{-1} and 25°C. The viscosity can therefore be ranked from pure DES to HPMCAS-embedded DES in increasing order. The API-containing pure DES and PVP-embedded DES showed viscosity values of 0.317 ± 0.088 Pa•s and 6.31 ± 0.03 Pa•s, in the given order at the shear rate of 0.1 s^{-1} and 25°C. The addition of the API to the HPMCAS-embedded DES exhibited a phase-separation (as discussed in the following Section 3.3.2), which made the rheology measurements inapplicable in this case. The viscosity of the pure DES increased 18-fold once 15% w/w of PVP was added. After the addition of 5% w/w HPMCAS, an increase of around 2863 times was observed compared to the pure DES. The significant increase in viscosity observed in the HPMCAS-embedded DES supports the argument that the mixture formed was a semi-solid gel. Furthermore, as there was a yield point with 2.31 ± 0.51 Pa determined from the flow curves of the HPMCAS-DES samples, a non-Newtonian rheological structure was evidenced. This gel showed shear-thinning properties as the viscosity decreased with increasing shear rate. Contrary to the HPMCAS formulation, the PVP-embedded DES and the pure DES formulations showed constant viscosities at increasing shear rates. The two formulations did not show yield points within the measurement window (shear rates of 0.1-100 s^{-1}). Consequently, they were both identified as Newtonian liquids, despite significant increases in viscosity when the PVP is added to the DES. In summary, the three formulations demonstrated different flow behaviour, with pure DES and the PVP-embedded DES being liquids, whilst the HPCMAS-embedded DES showed semi-solid gel-like flow behaviour.

3.3.2. Stability study of API-containing formulations

The stability of the API-loaded pure- and PEDES formulations was analysed according to weight changes observed in different storage conditions. These values were calculated in percent to represent the adsorption and desorption of water in the formulations. As expected, insignificant changes were observed in the case of the sealed vials stored at 23% relative humidity, suggesting that this method is a suitable way to store the formulations to minimize the interference of water. By contrast, open glass vials exhibited desorption when stored at 20% relative humidity, and adsorption at 40% relative humidity. Desorption values of 0.183 ± 0.008% for the pure DES, 0.302 ± 0.018% for the PVP-embedded DES, and 0.315 ± 0.033% for the HPMCAS embedded DES was noted. The adsorption of 4.23 ± 0.10% was recorded for pure DES with indomethacin, whilst the value being 3.71 ± 0.51% for the PVP-embedded, and 2.27 ± 0.64% for the HPMCAS-embedded DES carrying API. The adsorption data correspond to the findings discussed in Section 3.2, as hygroscopicity was most pronounced for the pure, and the PVP-embedded DES. Gelled structures have been shown to exhibit less water uptake due to the hindrance of water flow through the network, which could explain the lower hygroscopicity observed in the HPMCAS-PEDES (Fujiyabu et al., 2019). Nevertheless, the most drastic changes in the physical sample attributes were detected in the HPMCAS-containing DES with indomethacin. The sealed glass vials containing the API-loaded gel had turned into a physical mixture of a slightly opaque gel surrounded by a liquid layer as in Fig. 2 image (b). Once the glass was tilted, the liquid phase would start flowing whilst the gelled phase remained a static bulk at the bottom. On the other hand, a colour change was observed in the open samples stored in 40% relative humidity, which had turned orange. A collapsed solid structure was seen at the bottom of the glass surrounded by the orange liquid phase, as seen in Fig. 2 image (c). A lower volume of the separated liquid phase was observed in the sealed vial in comparison to the open stored glass vial. The separated liquid phase in the open sample also had lower viscosity, as the liquid would start to flow faster when tilted. To further assess the observed phase-separation, polarized light microscopy images (Olympus BX51, Tokyo, Japan) of the separated liquid phase are presented in Fig. 3. The images show droplets of darker shade encapsulating globular structures spotted in the separated liquid phase.

The phase separation observed shows the split of unidentified components into either a gelled semi-solid phase or a free-flowing liquid phase. The two phases had different levels of transparency, opacity and colour, suggesting that they have different compositions. The different colours are shown in the images in Fig. 2, where an orange liquid is clearly seen in image (c), as opposed to the more yellow liquid seen in (b). Fig. 3 shows that the separated liquid is not homogenous and thereby deems the sample as inadequate for further development. As a result, the PVP-embedded L-carnitine:ethylene glycol (1:4) DES with incorporated indomethacin was chosen as the final formulation candidate for additional characterization.

3.4. Further characterization of the PVP-PEDES candidate formulation

3.4.1. Molecular dynamics simulations

The molecular organization in DES has been a topic of much research and there seems to be no single uniform structural explanation for the interactions within a DES. The disordered hydrogen-bond interactions taking place between the various functional groups of the components within a DES, are often referred to as the “alphabet soup of hydrogen-bonds” (Ashworth et al., 2016). This liquid state is maintained stable

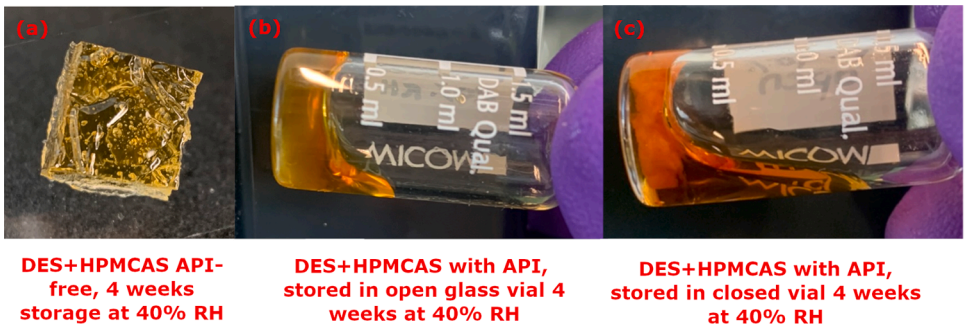

Fig. 2. Images demonstrating the phase separation observed in the HPMCAS-embedded DES before and after storage with API at 40% relative humidity for four weeks, in open and sealed glass vials. The image on the left (a) depicts the pure HPMCAS-PEDES, whilst (b) displays the sample stored in a hermetically sealed glass vial, and (c) shows the open stored sample, all after four weeks of storage in 40% relative humidity. Image (a) displays a transparent faint-yellow gel-structure carved into the shape of a rectangle, whilst image (b) shows an immobile opaque gel-phase at the bottom of the glass, surrounded by a separated viscous transparent liquid phase flowing on the side onto the glass wall in the tilted position. A collapsed solid structure, surrounded by a separated orange liquid, is seen at the bottom of the glass in photo (c).

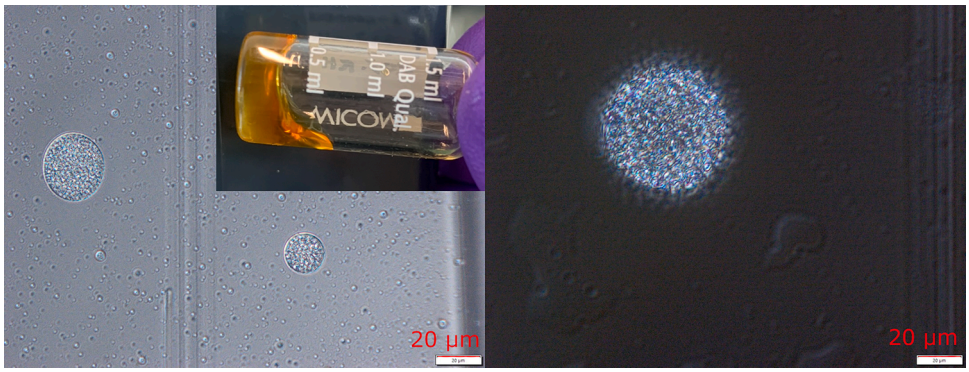

Fig. 3. Microscopic photos of the DES formulation embedded with 5% w/w HPMCAS loaded with indomethacin, after four weeks' storage in sealed glass vials at 40% relative humidity. Phase separation is observed as the syneresis of globular droplets of a darker shade are seen in the micrometre range.

regardless of the lack of a repetitive interacting structure and the presence of a consistent high-entropy state in the mixture. The high entropy of the structure overcomes an enthalpic energy of liquefaction as a mixture. To gain molecular insights into the structure of the selected PEDES, a full atomistic MD simulation was conducted. As a result, a 10 ns snapshot is displayed in Fig. 4, which only depicts the solvent molecules with ethylene glycol in blue and L-carnitine in conventional colours for the different atoms. Ethylene glycol molecules with their hydroxyl groups showed both hydrogen bond donating and accepting qualities, which provided a network of cohesive intermolecular bonds. L-carnitine also formed a network of hydrogen bonds with itself involving the carboxyl as well as hydroxyl groups; apart from these cohesive interactions, a further interacting hydrogen bonding network was observed between the two solvent types in which ethylene glycol primarily acted as the hydrogen bond donor and L-carnitine as acceptor. The solvent system appeared to harness a great number of molecular configurations to result in a mixing entropy that would greatly contribute to the successful formation of the given deep eutectic system.

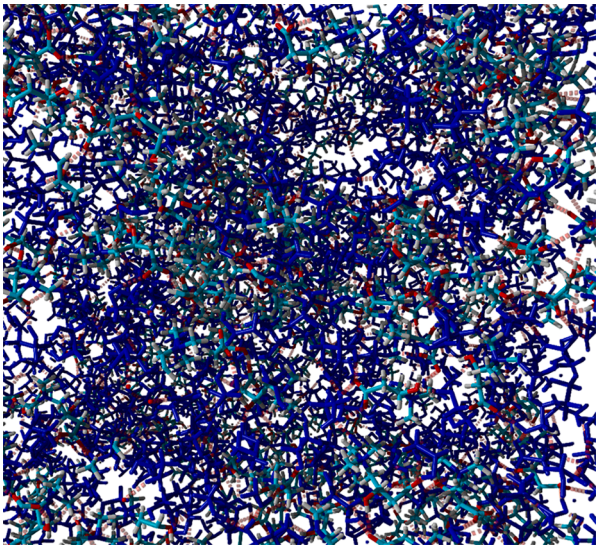

Fig. 4. Snapshot of a molecular dynamics simulation (10 ns, 298 K and 1 bar) exclusively showing the selected solvents (tube model) with ethylene glycol in blue for better discrimination from the other l-carnitine molecules. Hydrogen bonds are depicted as red dashes. Details are given in the text.

To emphasize the embedded polymer with drug, Fig. 5 shows the selected mixture by hiding the solvent molecules for clarity of presentation. Simulated polymer appeared to be well dispersed in the solvent and showed some coiling as well as overlapping of individual PVP oligomers. As for the active compound, indomethacin was to some extent freely dissolved wherein the solvent molecules exhibited both polar interactions/hydrogen bonding as well as hydrophobic interactions for solvation. Additionally, some cation-pi electron interactions were observed between the tertiary amine of carnitine and aromatic drug moieties, but due to the less frequent occurrence of this type of interaction, a contribution to the overall drug solvation was not expected to be relevant. Apart from free drug in solution, some indomethacin molecules were attached to the polymer, thereby showing primarily hydrophobic interactions. Moreover, such hydrophobic interactions were also found between some aggregated drug indomethacin molecules, mostly in the vicinity of polymer surface. Overall, the MD simulation provides the view that all components interacted with each other to some extent, and PVP showed no indication of a pronounced deswelling. Thus, the microscopic view mirrored the homogenous

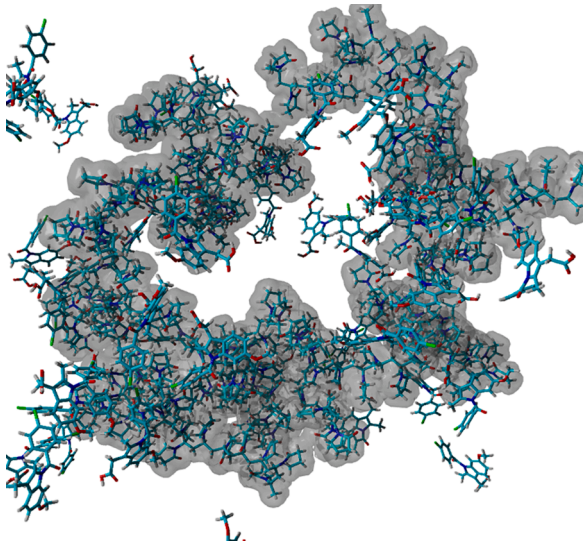

Fig. 5. Snapshot of a molecular dynamics (MD) simulation (10 ns, 298 K and 1 bar) in which the solvent molecules are hidden to depict solely the embedded PVP oligomers with dissolved or interacting indomethacin molecules (as tube model with the given molecular surface of PVP). Details are given in the text.

macroscopic appearance of the PEDES.

3.4.2. *Non-sink miniature-scale release test*

A non-sink miniature-scale release test was performed on the selected formulation of L-carnitine:ethylene glycol (1:4, molar ratio) with 15% w/w PVP and drug concentration corresponding to 80% of the equilibrium solubility. The release test was of particular interest as PEDES presents a novel supersaturating drug delivery system. It was a proof of concept for the type of *in vitro* drug release regarding the intended sustained drug supersaturation. To assess the supersaturation levels, further thermodynamic solubility tests in the release medium (phosphate buffer with a pH of 6.5) were conducted, as diluted components of the formulations could affect aqueous solubility. Therefore, drug solubility was determined in the "diluted DES:buffer" media, i.e., DES and buffer at a volumetric ratio of 1:10 v/v. As mentioned in Section 3.3, the API solubility in the phosphate buffer pH 6.5 was found to be 0.562 ± 0.005 mg/mL, and 1.16 ± 0.01 mg/mL in the diluted DES:buffer (1:10 v/v) media. The release kinetics obtained from the two API-incorporated DES formulations, with or without PVP (PEDES or DES, respectively) are displayed in Fig. 6 and the respective solubility values in pure buffer and buffer with DES are given for comparison.

As expected, the trend of the curve obtained from the PVP-based PEDES maintained a higher supersaturation level in the two-hour measurement time compared to the kinetics obtained from the pure DES formulation. The area under the curve (AUC) determined for the release curve of the pure DES was 575.5 ± 26.2 min • mg/mL, whilst the value was 1276.1 ± 52.7 min • mg/mL for the PEDES. An exponential decline in the concentration of dissolved API in the pure DES formulation was noted after the peak concentration at 30 min until the end of the experiment (120 min in total). A clear reduction in the extent of precipitation was observed when polymer was incorporated, since higher dissolved API concentrations were measured in the polymer-embedded sample during the experiment. The highest concentration for both release curves was measured after 30 minutes: 11.39 ± 0.07 mg/mL for PEDES and 7.98 ± 0.16 mg/mL in the case of pure DES formulation. These correspond to solubility values 20.3 and 14.2 times higher than the equilibrium solubility of the API in the pure release medium (phosphate buffer pH 6.5), and 9.8 and 6.9 times higher than the equilibrium solubility of indomethacin in the blank release medium (DES:phosphate buffer pH 6.5 1:10 v/v). Thus, pronounced supersaturation was noted for both formulations but PEDES with the embedded PI demonstrated relatively higher concentrations *in vitro*. The mechanism behind the precipitation inhibition obtained from the application of a PI was likely due to steric hindrance on the level of crystal nucleation and growth (Bauer-Brandl & Brandl, 2019; Price et al., 2019; Warren et al., 2010). This could be linked to the findings of the MD simulations, as the coiled PVP played a role in maintaining spatial distance between the indomethacin molecules, thereby blocking nucleation and crystal growth. This was also supported by the observation of hydrophobic interactions between the polymer entity and some of the API molecules, providing distance between the individual API molecules. The resulting supersaturation combined with the sustained supersaturation recorded over time in the PEDES displayed suitable "spring & parachute" concentration kinetics, which was deemed a successful result regarding further development of PEDES as a novel bio-enabling formulation.

4. Conclusion

Previous research has shown that DESs typically possess high solubilization capacities for different poorly soluble compounds (Fourmentin et al., 2021) and that some have the potential to become a bio-enabling formulation (Palmelund, Eriksen, et al., 2021). Accordingly, this study presents the PEDES approach for which the PI is directly

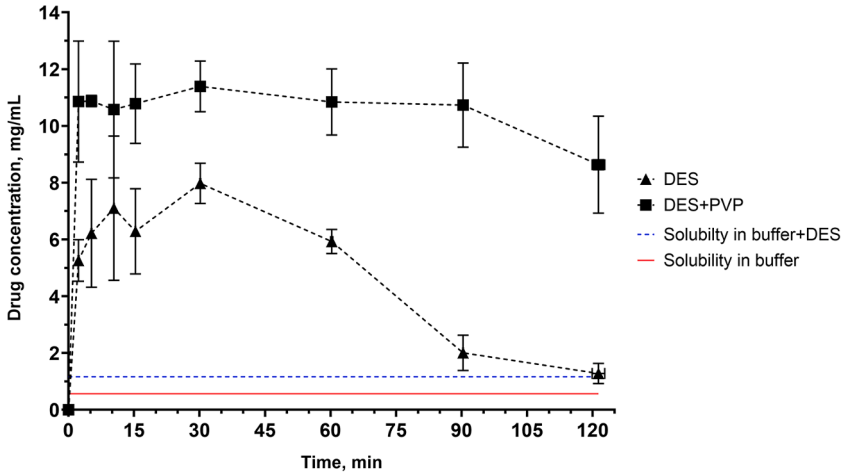

Fig. 6. Kinetic indomethacin concentrations obtained from the non-sink release test from the pure DES formulation (▲) and the PEDES with 15% w/w PVP (■). Equilibrium solubilities in diluted DES:buffer media (DES:phosphate buffer pH 6.5, 1:10 v/v) and buffer (phosphate buffer pH 6.5) are marked by the blue dashed-line (- - -) and the red line (▬), respectively.

incorporated in a DES. Following a broad screening, a selected DES made of L-carnitine and ethylene glycol at the molar ratio of 1:4 was successfully mixed with 15% w/w PVP. The impact of water and humidity, along with the formulation's rheological character, was characterized and compared to another PEDES using the same DES but with 5% w/w HPMCAS as the PI. The latter was not considered for further formulation development due to physical instability. The indomethacin *in vitro* release showed a suitable "spring & parachute" effect with generally higher kinetic concentrations compared to DES without polymer. These findings are promising, in that PIs can be embedded in a DES to formulate a novel type of SDDS. The outstanding solubility improvement and supersaturation levels are further evidence that DES and especially PEDES are of pharmaceutical interest, for example regarding preclinical or clinical formulations and eventually even for market formulation development. The final dosage form could be then either a liquid-filled capsule or a bulk solution of PEDES that is further dried and downstream processed to obtain a solid dosage form with drug in a preferably non-crystalline form. Future research on PEDES with different drugs and PIs will show how this novel type of bio-enabling formulation will compare to other more established formulation approaches.

Data statement

The presented experimental data can be obtained from the corresponding author on request.

Author contribution

Shaida Panbachi: Research in the laboratory and original draft preparation. **Josef Beranek:** Conceptualization, reviewing and editing. **Martin Kuentz:** Supervisor, conceptualization, molecular modeling, reviewing, and editing.

Funding and role of funding source

This work has received funding from the European Union's Horizon 2020 research and innovation program the Marie Skłodowska-Curie grant agreement No 955756. (InPharma). The funding source has had no involvement in the study design, in the collection, analysis and interpretation of data, in the writing of the report, nor in the decision to submit the article for publication.

Declaration of Competing Interest

The authors declare that they have no known competing financial interests or personal relationships that could have appeared to influence the work reported in this paper.

Data availability

Data will be made available on request.

Acknowledgments

Natalia Magda Zlotkowska is thanked and acknowledged for her valiant efforts and assistance in the setup of the time-domain NMR.

References

Abbott, A., Capper, G., Davies, D., Rasheed, R.K., Tambyrajah, V., 2002. Novel solvent properties of choline chloride/urea mixtures. Chem. Commun. (Cambridge) 70–71.

Abranches, D. O., & Coutinho, J. A. P. (2023). Everything you wanted to know about deep eutectic solvents but were afraid to be told. 10.1146/annurev-chembioeng.

Abreu-Villela, R., Kuentz, M., Caraballo, I., 2019. Benefits of fractal approaches in solid dosage form development. Pharm. Res. 36 (11), 1–13. https://doi.org/10.1007/S11095-019-2685-5/FIGURES/5.

Ahmed Rahma, W.S., Mjalli, F.S., Al-Wahaibi, T., Al-Hashmi, A.A, 2017. Polymeric-based deep eutectic solvents for effective extractive desulfurization of liquid fuel at ambient conditions. Chem. Eng. Res. Des. 120, 271–283. https://doi.org/10.1016/J.CHERD.2017.02.025.

Aroso, I.M., Silva, J.C., Mano, F., Ferreira, A.S.D., Dionísio, M., Sá-Nogueira, I., Barreiros, S., Reis, R.L., Paiva, A., Duarte, A.R.C., 2016a. Dissolution enhancement of active pharmaceutical ingredients by therapeutic deep eutectic systems. Eur. J. Pharm. Biopharm. 98, 57–66. https://doi.org/10.1016/J.EJPB.2015.11.002.

Aroso, I.M., Silva, J.C., Mano, F., Ferreira, A.S.D., Dionísio, M., Sá-Nogueira, I., Barreiros, S., Reis, R.L., Paiva, A., Duarte, A.R.C., 2016b. Dissolution enhancement of active pharmaceutical ingredients by therapeutic deep eutectic systems. Eur. J. Pharm. Biopharm. 98, 57–66. https://doi.org/10.1016/J.EJPB.2015.11.002.

Ashworth, C.R., Matthews, R.P., Welton, T., Hunt, P.A., 2016. Doubly ionic hydrogen bond interactions within the choline chloride-urea deep eutectic solvent. Phys. Chem. Chem. Phys. 18, 18145. https://doi.org/10.1039/c6cp02815b.

Bauer-Brandl, A., Brandl, M., 2019. 2. Solubility and supersaturation. Solubility Pharm. Chem. 27–70. https://doi.org/10.1515/9783110559835-002/HTML.

Benvenutti, L., Zielinski, A.A.F., Ferreira, S.R.S., 2019. Which is the best food emerging solvent: IL, DES or NADES? Trends Food Sci. Technol. 90, 133–146. https://doi.org/10.1016/J.TIFS.2019.06.003.

Bevernage, J., Brouwers, J., Brewster, M.E., Augustijns, P., 2013. Evaluation of gastrointestinal drug supersaturation and precipitation: Strategies and issues. Int. J. Pharm. 453 (1), 25–35. https://doi.org/10.1016/J.IJPHARM.2012.11.026.

Boyd, B.J., Bergström, C.A.S., Vinarov, Z., Kuentz, M., Brouwers, J., Augustijns, P., Brandl, M., Bernkop-Schnürch, A., Shrestha, N., Préat, V., Müllertz, A., Bauer-Brandl, A., Jannin, V., 2019. Successful oral delivery of poorly water-soluble drugs both depends on the intraluminal behavior of drugs and of appropriate advanced drug delivery systems. Eur. J. Pharm. Sci. 137, 104967 https://doi.org/10.1016/J.EJPS.2019.104967.

Buckley, S.T., Frank, K.J., Fricker, G., Brandl, M., 2013. Biopharmaceutical classification of poorly soluble drugs with respect to 'enabling formulations. Eur. J. Pharm. Sci. 50 (1), 8–16. https://doi.org/10.1016/J.EJPS.2013.04.002.

Chakraborty, S., Chormale, J.H., Bansal, A.K., 2021. Deep eutectic systems: an overview of fundamental aspects, current understanding and drug delivery applications. Int. J. Pharm. 610, 121203 https://doi.org/10.1016/J.IJPHARM.2021.121203.

Dai, Y., van Spronsen, J., Witkamp, G.J., Verpoorte, R., Choi, Y.H., 2013. Natural deep eutectic solvents as new potential media for green technology. Anal. Chim. Acta 766, 61–68. https://doi.org/10.1016/J.ACA.2012.12.019.

Essmann, U., Perera, L., Berkowitz, M.L., Darden, T., Lee, H., Pedersen, L.G., 1998. A smooth particle mesh Ewald method. J. Chem. Phys. 103 (19), 8577. https://doi.org/10.1063/1.470117.

Faggian, M., Sut, S., Perissutti, B., Baldan, V., Grabnar, I., & Dall'acqua, S. (2016). Molecules Natural Deep Eutectic Solvents (NADES) as a tool for bioavailability improvement: pharmacokinetics of rutin dissolved in proline/glycine after oral administration in rats: possible application in nutraceuticals. 10.3390/molecules21111531.

Fourmentin, S., Costa Gomes, M., & Lichtfouse, E. (2021). Deep eutectic solvents for medicine, gas solubilization and extraction of natural substances. 312.

Francisco, M., van den Bruinhorst, A., Kroon, M.C., 2013. Low-transition-temperature mixtures (LTTMs): a new generation of designer solvents. Angew. Chem. - Int. Ed. 52 (11), 3074–3085. https://doi.org/10.1002/ANIE.201207548.

Friesen, D.T., Shanker, R., Crew, M., Smithey, D.T., Curatolo, W.J., Nightingale, J.A.S., 2008. Hydroxypropyl methylcellulose acetate succinate-based spray-dried dispersions: an overview. Mol. Pharm. 5 (6), 1003–1019. https://doi.org/10.1021/MP8000793.

Fujiyabu, T., Li, X., Chung, U.il, Sakai, T., 2019. Diffusion behavior of water molecules in hydrogels with controlled network structure. Macromolecules 52 (5), 1923–1929. https://doi.org/10.1021/ACS.MACROMOL.8B02488/SUPPL_FILE/MA8B02488_SI_001.PDF.

García-Argüelles, S., Serrano, M.C., Gutiérrez, M.C., Ferrer, M.L., Yuste, L., Rojo, F., del Monte, F., 2013. Deep eutectic solvent-assisted synthesis of biodegradable polyesters with antibacterial properties. Langmuir 29 (30), 9525–9534. https://doi.org/10.1021/LA401353R/SUPPL_FILE/LA401353R_SI_001.PDF.

Guo, Z., Ma, M., Wang, T., Chang, D., Jiang, T., Wang, S., 2011. A kinetic study of the polymorphic transformation of nimodipine and indomethacin during high shear granulation. AAPS PharmSciTech 12 (2), 610. https://doi.org/10.1208/S12249-011-9628-8.

Hansen, B.B., Spittle, S., Chen, B., Poe, D., Zhang, Y., Klein, J.M., Horton, A., Adhikari, L., Zelovich, T., Doherty, B.W., Gurkan, B., Maginn, E.J., Ragauskas, A., Dadmun, M., Zawodzinski, T.A., Baker, G.A., Tuckerman, M.E., Savinell, R.F., Sangoro, J.R., 2021. Deep eutectic solvents: a review of fundamentals and applications. Chem. Rev. 121 (3), 1232–1285. https://doi.org/10.1021/acs.chemrev.0c00385.

Hiremath, P., Nuguru, K., Agrahari, V., 2019. Material attributes and their impact on wet granulation process performance. Handbook of Pharmaceutical Wet Granulation: Theory and Practice in a Quality by Design Paradigm, pp. 263–315. https://doi.org/10.1016/B978-0-12-810460-6.00012-9.

Huber, V., Hioe, J., Touraud, D., Kunz, W., 2022. Uncovering the curcumin solubilization ability of selected natural deep eutectic solvents based on quaternary ammonium compounds. J. Mol. Liq. 361, 119661 https://doi.org/10.1016/J.MOLLIQ.2022.119661.

Jakalian, A., Jack, D.B., Bayly, C.I., 2002. Fast, efficient generation of high-quality atomic charges. AM1-BCC model: II. Parameterization and validation. J. Comput. Chem. 23 (16), 1623–1641. https://doi.org/10.1002/JCC.10128.

Jeliński, T., Przybyłek, M., & Cysewski, P. (2019). Natural deep eutectic solvents as agents for improving solubility, stability and delivery of curcumin. 10.1007/s11095-019-2643-2.

Jeong, K.M., Ko, J., Zhao, J., Jin, Y., Yoo, D.E., Han, S.Y., Lee, J., 2017. Multi-functioning deep eutectic solvents as extraction and storage media for bioactive natural products that are readily applicable to cosmetic products. J. Cleaner Prod. 151, 87–95. https://doi.org/10.1016/J.JCLEPRO.2017.03.038.

Kaur, S., Kumari, M., Kashyap, H.K., 2020. Microstructure of deep eutectic solvents: current understanding and challenges. J. Phys. Chem. B 124 (47), 10601–10616. https://doi.org/10.1021/ACS.JPCB.0C07934.

Krieger, E., Vriend, G., 2014. YASARA View - molecular graphics for all devices - from smartphones to workstations. Bioinformatics 30 (20), 2981–2982. https://doi.org/10.1093/BIOINFORMATICS/BTU426.

Kuentz, M., 2019. Drug supersaturation during formulation digestion, including real-time analytical approaches. Adv. Drug. Deliv. Rev. 142, 50–61. https://doi.org/10.1016/J.ADDR.2018.11.003.

Kuentz, M., Egloff, P., Röthlisberger, D., 2006. A technical feasibility study of surfactant-free drug suspensions using octenyl succinate-modified starches. Eur. J. Pharm. Biopharm. 63 (1), 37–43. https://doi.org/10.1016/J.EJPB.2005.10.004.

Kuentz, M., Rothenhäusler, B., Röthlisberger, D., 2006. Time domain 1H NMR as a new method to monitor softening of gelatin and HPMC capsule shells. Drug Dev. Ind. Pharm. 32 (10), 1165–1173. https://doi.org/10.1080/03639040600683659.

Lee, J.S., 2017. Deep eutectic solvents as versatile media for the synthesis of noble metal nanomaterials. Nanotechnol. Rev. 6 (3), 271–278. https://doi.org/10.1515/NTREV-2016-0106/ASSET/GRAPHIC/J_NTREV-2016-0106_FIG_005.JPG.

Li, Z., Lee, P.I., 2016. Investigation on drug solubility enhancement using deep eutectic solvents and their derivatives. Int. J. Pharm. 505 (1–2), 283–288. https://doi.org/10.1016/J.IJPHARM.2016.04.018.

Lu, C., Cao, J., Wang, N., Su, E., 2016. Significantly improving the solubility of non-steroidal anti-inflammatory drugs in deep eutectic solvents for potential non-aqueous liquid administration. MedChemComm 7 (5), 955–959. https://doi.org/10.1039/C5MD00551E.

Machado, A.H.E., Kokubo, T., Dujovny, G., Jones, B., Scialdone, C., Bravo, R., Kuentz, M., 2016. A microstructural study of water effects in lipid-based pharmaceutical formulations for liquid filling of capsules. Eur. J. Pharm. Sci. 90, 64–75. https://doi.org/10.1016/J.EJPS.2016.04.035.

Marcus, Y., 2019. Deep Eutectic Solvents. Deep Eutectic Solvents. https://doi.org/10.1007/978-3-030-00608-2.

Martins, M.A.R., Pinho, S.P., Coutinho, J.A.P., 2019. Insights into the nature of eutectic and deep eutectic mixtures. J. Solution Chem. 48 (7), 962–982. https://doi.org/10.1007/s10953-018-0793-1.

Mathews, C.D.C., Sugano, K., 2010. Supersaturable formulations. Drug Deliv. Syst. 25 (4), 371–374. https://doi.org/10.2745/DDS.25.371.

Morrison, H.G., Sun, C.C., Neervannan, S., 2009. Characterization of thermal behavior of deep eutectic solvents and their potential as drug solubilization vehicles. Int. J. Pharm. 378 (1–2), 136–139. https://doi.org/10.1016/J.IJPHARM.2009.05.039.

Palmelund, H., Eriksen, J.B., Bauer-Brandl, A., Rantanen, J., Löbmann, K., 2021. Enabling formulations of aprepitant: *in vitro* and *in vivo* comparison of nanocrystalline, amorphous and deep eutectic solvent based formulations. Int. J. Pharm. X 3, 100083. https://doi.org/10.1016/J.IJPX.2021.100083.

Palmelund, H., Rantanen, J., Löbmann, K., 2021. Deliquescence behavior of deep eutectic solvents. Appl. Sci. 11, 1601. https://doi.org/10.3390/app11041601.

Pedro, S.N., Freire, C.S.R., Silvestre, A.J.D., Freire, M.G., 2020. The role of ionic liquids in the pharmaceutical field: an overview of relevant applications. Int. J. Mol. Sci. 21 (21), 1–50. https://doi.org/10.3390/IJMS21218298.

Potticary, J., Hall, C., Hamilton, V., McCabe, J.F., Hall, S.R., 2020. Crystallisation from volatile deep eutectic solvents. Cryst. Growth Des. 20 (5), 2877–2884. https://doi.org/10.1021/ACS.CGD.0C00399.

Price, D.J., Ditzinger, F., Koehl, N.J., Jankovic, S., Tsakiridou, G., Nair, A., Holm, R., Kuentz, M., Dressman, J.B., Saal, C., 2019. Approaches to increase mechanistic understanding and aid in the selection of precipitation inhibitors for supersaturating formulations – a PEARRL review. J. Pharm. Pharmacol. 71 (4), 483–509. https://doi.org/10.1111/JPHP.12927.

Rahman, M.S., Roy, R., Jadhav, B., Hossain, M.N., Halim, M.A., Raynie, D.E., 2021. Formulation, structure, and applications of therapeutic and amino acid-based deep eutectic solvents: an overview. J. Mol. Liq. 321 https://doi.org/10.1016/J.MOLLIQ.2020.114745.

Ramón, D.J., Guillena, G., 2019. Deep eutectic solvents: synthesis, properties, and applications. Deep Eutectic Solvents: Synthesis, Properties, and Applications, pp. 1–370. https://doi.org/10.1002/9783527818488.

Şahin, S., Kurtulbaş, E., Bilgin, M., ¸ahin, S. S., & Kurtulbas¸, K., 2023. Special designed deep eutectic solvents for the recovery of high added-value products from olive leaf: a sustainable environment for bioactive materials. 10.1080/10826068.2020.1824162.

Sanchez-Fernandez, A., Hammond, O.S., Edler, K.J., Arnold, T., Doutch, J., Dalgliesh, R. M., Li, P., Ma, K., Jackson, A.J., 2018. Counterion binding alters surfactant self-assembly in deep eutectic solvents. Phys. Chem. Chem. Phys. 20 (20), 13952–13961. https://doi.org/10.1039/C8CP01008K.

Sanchez-Fernandez, A., Leung, A.E., Kelley, E.G., Jackson, A.J., 2021. Complex by design: hydrotrope-induced micellar growth in deep eutectic solvents. J. Colloid Interface Sci. 581, 292–298. https://doi.org/10.1016/J.JCIS.2020.07.077.

Sapir, L., Stanley, C.B., Harries, D., 2016. Properties of polyvinylpyrrolidone in a deep eutectic solvent. J. Phys. Chem. A 120 (19), 3253–3259. https://doi.org/10.1021/ACS.JPCA.5B11927/SUPPL_FILE/JP5B11927_SI_001.PDF.

Shah, S., Date, A., Holm, R., 2019. Strategies for the formulation development of poorly soluble drugs via oral route. Innovative Dosage Forms: Design and Development at Early Stage, pp. 49–89. https://doi.org/10.1002/9783527812172.CH2.

Shakeel, F., Alanazi, F.K., Alsarra, I.A., Haq, N., 2013. Solubility prediction of indomethacin in PEG 400 + water mixtures at various temperatures. J. Mol. Liq. 188, 28–32. https://doi.org/10.1016/J.MOLLIQ.2013.09.013.

Skowrońska, D., Wilpiszewska, K., 2022. Deep eutectic solvents for starch treatment. Polymers 14 (2). https://doi.org/10.3390/POLYM14020220.

Sugano, K., 2012. Enabling formulations. Biopharmaceutics Modeling and Simulations, pp. 347–378. https://doi.org/10.1002/9781118354339.CH11.

Sut, S., Faggian, M., Baldan, V., Poloniato, G., Castagliuolo, I., Grabnar, I., Perissutti, B., Brun, P., Maggi, F., Voinovich, D., Peron, G., & Dall, S. (2017). Molecules Natural Deep Eutectic Solvents (NADES) to enhance berberine absorption: an *in vivo* pharmacokinetic study. 10.3390/molecules22111921.

Taylor, L.S., Zhang, G.G.Z., 2016. Physical chemistry of supersaturated solutions and implications for oral absorption. Adv. Drug. Deliv. Rev. 101, 122–142. https://doi.org/10.1016/J.ADDR.2016.03.006.

Tomé, L.C., Mecerreyes, D., 2020. Emerging ionic soft materials based on deep eutectic solvents. J. Phys. Chem. B 124 (39), 8465–8478. https://doi.org/10.1021/ACS.JPCB.0C04769/ASSET/IMAGES/MEDIUM/JP0C04769_0011.GIF.

Umerska, A., Bialek, K., Zotova, J., Skotnicki, M., Tajber, L., 2020. Anticrystal engineering of ketoprofen and ester local anesthetics: ionic liquids or deep eutectic mixtures? Pharmaceutics 12 (4). https://doi.org/10.3390/PHARMACEUTICS12040368.

Vranić, E., Uzunović, A, 2010. Dissolution studies of physical mixtures of indomethacin with alpha-and gamma-cyclodextrins edina vranić and alija uzunović: dissolution studies of physical mixtures of indomethacin with alpha⌣ and gamma⌣cyclodextrins. Bosn. J. Basic Med. Sci. 10 (3).

Wang, J., Wolf, R.M., Caldwell, J.W., Kollman, P.A., Case, D.A., 2004. Development and testing of a general amber force field. J. Comput. Chem. 25 (9), 1157–1174. https://doi.org/10.1002/JCC.20035.

Warren, D. B., Benameur, H., Porter, C. J. H., & Pouton, C. W. (2010). Using polymeric precipitation inhibitors to improve the absorption of poorly water-soluble drugs: a mechanistic basis for utility. 18(10), 704–731. 10.3109/1061186X.2010.525652.

Zhang, K., Ren, S., Hou, Y., Wu, W., 2017. Efficient absorption of SO2 with low-partial pressures by environmentally benign functional deep eutectic solvents. J. Hazard. Mater. 324, 457–463. https://doi.org/10.1016/J.JHAZMAT.2016.11.012.